# Optimal Periodic Orbits of Chaotic Systems

Brian R. Hunt[1,*] and Edward Ott[2]
[1]*Institute for Physical Science and Technology, University of Maryland, College Park, Maryland 20742*
[2]*Institute for Plasma Research, Institute for Systems Research, and Departments of Electrical Engineering and of Physics, University of Maryland, College Park, Maryland 20742*
(Received 24 October 1995)

Invariant sets embedded in a chaotic attractor can generate time averages that differ from the average generated by typical orbits on the attractor. Motivated by two different topics (namely, controlling chaos and riddled basins of attraction), we consider the question of which invariant set yields the largest (optimal) value of an average of a given smooth function of the system state. We present numerical evidence and analysis which indicate that the optimal average is typically achieved by a low period unstable periodic orbit embedded in the chaotic attractor.

PACS numbers: 05.45.+b

Many questions concerning dynamical behavior are addressed by consideration of the long-time average of a function $F$ of the state vector $x$,

$$\langle F \rangle = \lim_{t \longrightarrow \infty} \frac{1}{t} \int_0^t F(x(t'))\, dt', \tag{1a}$$

$$\langle F \rangle = \lim_{t \longrightarrow \infty} \frac{1}{t} \sum_{t'=1}^{t} F(x_{t'}), \tag{1b}$$

where $t$ denotes time and is either continuous [Eq. (1a)] or discrete [Eq. (1b)].

In this paper we consider systems such that, for *typical* choices of the initial $x$, the trajectory generated by the dynamical system is chaotic and has a well-defined long-time average (1). (Here "typical" is with respect to the Lebesgue measure of initial conditions in state space.) We note, however, that atypical initial conditions may generate orbits embedded in the chaotic attractor that have different values for $\langle F \rangle$ than typical orbits. For example, consider a chaotic attractor with a basin of attraction $B$. Even though there is a set of initial conditions in $B$ all yielding the *same* value for $\langle F \rangle$, and the state space volume (Lebesgue measure) of these initial conditions is equal to the entire volume of $B$, there is still a zero volume set of initial conditions ("atypical" initial conditions) whose orbits asymptote to sets within the chaotic attractor but for which $\langle F \rangle$ is different from the average attained by typical orbits. A familiar case where this happens is when the initial condition is placed exactly on an unstable periodic orbit embedded in a chaotic attractor (or on the stable manifold of the unstable periodic orbit).

The question we address is the following. *Which (atypical) orbit on the attractor yields the largest value of $\langle F \rangle$?* To our knowledge this question has not been previously addressed, yet it is fundamental to at least two important problem areas of current interest:

*(a) Controlling chaos.*—In one often used method [1] for the control of chaos by use of small controls the strategy is to first identify several low period unstable periodic orbits embedded in the chaotic attractor. One then determines the system performance that would apply if each of the various determined unstable periodic orbits were actually followed by the system. In many cases the system performance can be quantified as the value of some time average $\langle F \rangle$, as in Eq. (1). One then selects an orbit yielding performance that is best and feedback stabilizes that orbit. A question that might be asked is whether one can obtain much better performance by looking exhaustively at higher period orbits or by considering stabilization of atypical *nonperiodic* orbits embedded in the chaotic attractor.

*(b) Bifurcation to riddled basins of attraction.*—Recently a new type of basin of attraction has been found. This new basin type is called a *riddled* basin [2,3], and has the property that any point in the basin has points in another attractor's basin arbitrarily close to it (the basin, although of positive volume, has no interior). This type of behavior can be present in dynamical systems that possess an invariant manifold $M$ and a chaotic attractor in that manifold. An interesting basic question is that of how a nonriddled basin for the chaotic attractor on $M$ becomes riddled as a system parameter is varied (i.e., the bifurcation to a riddled basin) [4]. This bifurcation occurs [5,6] when the Lyapunov exponent for perturbations transverse to $M$, maximized over all invariant sets in the chaotic attractor, first becomes positive. Thus the study of this bifurcation again focuses on the invariant set maximizing an average (i.e., the transverse Lyapunov exponent) [5–7].

To begin we consider a simple example, namely the doubling transformation

$$x_{t+1} = 2x_t (\mathrm{mod}\ 1), \tag{2}$$

and for $F$ we take

$$F_\gamma(x) = \cos[2\pi(x - \gamma)]. \tag{3}$$

Although some of the results we observe for Eqs. (2) and (3) are model specific, we claim that Eqs. (2) and (3) also yield essential behaviors that should be expected

 0031-9007/96/76(13)/2254(4)$10.00 © 1996 The American Physical Society

in general for low-dimensional chaotic systems. A main point will be that the optimal average is typically achieved by a low period periodic orbit [8].

For each of $10^5$ evenly spaced values of $\gamma$, we tested the value of $\langle F_\gamma \rangle$ for all periodic orbits of the map (2) with periods 1 to 24. There are on the order of $10^6$ such orbits. Figure 1 shows the period of the orbit that maximizes $\langle F_\gamma \rangle$ for Eqs. (2) and (3) as a function of the phase angle $\gamma$. The third column of Table I gives the fraction $f(p)$ of phase values $\gamma$ for which a period $p$ orbit maximizes $\langle F_\gamma \rangle$. For example, if $\gamma$ is chosen at random in $[0, 1]$, then over 93% of the time, the optimal periodic orbit does not exceed 7 in period, and more than half the time the optimal orbit's period is 1, 2, or 3. The second column in Table I gives a conjectured asymptotic prediction of the fraction $f(p)$ of the time a period $p$ orbit maximizes $\langle F_\gamma \rangle$ if $\gamma$ is chosen at random in $[0, 1]$,

$$f(p) = Kp2^{-p}\phi(p). \tag{4}$$

Here $\phi(p)$ is the Euler function, which is defined as the number of integers between 1 and $p$ (inclusive) that are relatively prime to $p$ [e.g., the numbers 1, 5, 7, and 11 are relatively prime to 12, and so $\phi(12) = 4$]. Thus $\phi(p) \leq p - 1$ for $p \geq 2$, and $\phi(p) = p - 1$ if $p$ is a prime. The factor $K$ is a fitting parameter, which we choose to be $1/6$ in this example. We see from Table I and the data plotted as diamonds in Fig. 2 that Eq. (4) agrees very well with the numerical results for large $p$ [the straight line in Fig. 2 has slope $-\log 2$ and, for the plotted diamonds, the vertical axis is the logarithm of the numerically computed $f(p)$ divided by $p\phi(p)$]. From Table I, the agreement with Eq. (4) is better than 5% for $p > 5$. Note that Eq. (4) apparently has nothing to do with the precise choice of the function $F_\gamma$ in Eq. (3). We believe that Eq. (4) is a good approximation for typical smooth functions with a single maximum whose parameter dependence consists of a phase shift. Tests using other quadratic maximum, single humped functions [e.g., $F_\gamma(x) = -(x - \gamma)^2$] in place of Eq. (3) confirm this.

TABLE I. Numerical results for doubling map (2).

| | Theory | Eq. (3) | | Eq. (5) | |
|---|---|---|---|---|---|
| $p$ | $f(p)$ | $f(p)$ | $f_{90\%}(p)$ | $f(p)$ | $f_{90\%}(p)$ |
| 1 | 0.0833 | 0.299 | 0.333 | 0.230 | 0.258 |
| 2 | 0.0833 | 0.160 | 0.212 | 0.163 | 0.175 |
| 3 | 0.125 | 0.176 | 0.294 | 0.186 | 0.234 |
| 4 | 0.0833 | 0.0985 | 0.143 | 0.0850 | 0.110 |
| 5 | 0.104 | 0.116 | 0.0180 | 0.136 | 0.169 |
| 6 | 0.0313 | 0.0310 | 0 | 0.0350 | 0.0473 |
| 7 | 0.0547 | 0.0573 | 0 | 0.0427 | 0.00664 |
| 8 | 0.0208 | 0.0211 | 0 | 0.0583 | 0.00031 |
| 9 | 0.0176 | 0.0178 | 0 | 0.0244 | 0 |
| 10 | 0.00651 | 0.00644 | 0 | 0.00697 | 0 |
| 11 | 0.00895 | 0.00918 | 0 | 0.0164 | 0 |
| 12 | 0.00195 | 0.00196 | 0 | 0.00516 | 0 |
| 13 | 0.00317 | 0.00324 | 0 | 0.00446 | 0 |
| 14 | 0.00085 | 0.00084 | 0 | 0.00389 | 0 |
| 15 | 0.00061 | 0.00062 | 0 | 0.00105 | 0 |
| 16–24 | 0.00091 | 0.00092 | 0 | 0.00167 | 0 |

Not only are low period orbits most often optimal, but, even when a somewhat higher period orbit is optimal, it apparently leads only to a relatively small increase in $\langle F_\gamma \rangle$ as compared to a lower period orbit. This point is emphasized by the fourth column in Table I, which gives the fraction of the $\gamma$ values such that the lowest period orbit that yields a value of $\langle F_\gamma \rangle$ within 90% of the maximum value has period $p$. Thus, for this example, if one is willing to settle for 90% of optimal, one *never* has to go above period 5. Also for over 83% of the $\gamma$ values it suffices to consider only period 1, 2, and 3. The relatively small increase of $\langle F_\gamma \rangle$ achieved by going to a higher period is also evident from the plots of $\langle F_\gamma \rangle_p$ vs $\gamma$, where $\langle F_\gamma \rangle_p$ denotes the average of $F_\gamma$ over the period $p$ orbit that is optimal from among all period $p$ orbits.

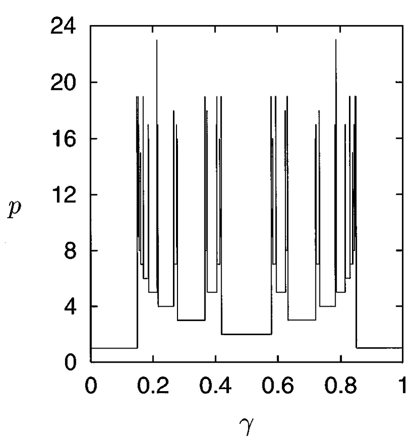


Fig. 1. Period that optimizes $\langle F_\gamma \rangle$ as a function of $\gamma$ for the doubling map (2) and function (3).

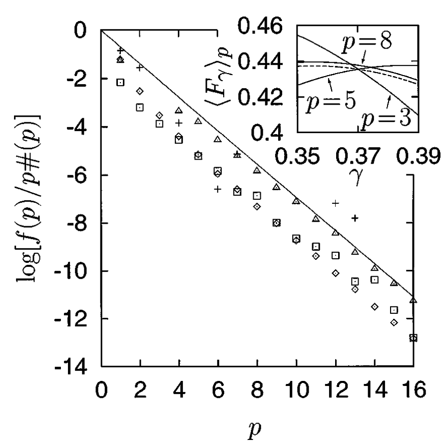


Fig. 2. Graph of $\log[f(p)/p\#(p)]$ vs $p$. The straight line has slope $-\log 2$. Inset shows $\langle F_\gamma \rangle_p$ vs $\gamma$ for $p = 3, 5, 8$.

For example, the $\gamma$ region near $\gamma \approx 0.37$ (cf. Fig. 1) has $p = 3$ and $p = 5$ intervals with a smaller $p = 8$ interval in between. A plot of $\langle F_\gamma \rangle_p$ for $p = 3, 5, 8$ in this region is shown in the inset in Fig. 2. The weighted average $(5\langle F_\gamma \rangle_5 + 3\langle F_\gamma \rangle_3)/(5 + 3)$ is shown as a dashed curve. Note that $\langle F_\gamma \rangle_8$ closely follows this average but is slightly above it. Thus $\langle F_\gamma \rangle_8$ is slightly larger than both $\langle F_\gamma \rangle_3$ and $\langle F_\gamma \rangle_5$ in a small region near $\gamma \approx 0.37$.

It is also interesting to note the Farey tree structure present in Fig. 1; the periods follow the pattern of the denominators in the Farey construction of the rational numbers. That is, between any two $\gamma$ intervals with optimal orbits of periods $p_a$ and $p_b$ and only higher periods associated with any intervening $\gamma$ intervals, there is a smaller $\gamma$ interval of period $p_a + p_b$ in between, and all other $\gamma$ intervals in between have periods higher than $p_a + p_b$. This is illustrated by Fig. 1. For example, consider the $\gamma$ interval $[0.35, 0.45]$. Between the period 3 interval and the period 2 interval there is a period 5 interval. Between the 3 and the 5 there is an 8, between the 5 and the 2 there is a 7, and so on. Numerically we find an exponential decrease, as $p$ increases, of the total length of the $\gamma$ intervals with period at least $p$ (this can be discerned from the data in Table I). Noting this and thinking of optimal nonperiodic orbits as being created in the limit as the Farey tree level approaches infinity [9], we infer that optimal nonperiodic orbits typically do not occur on a positive Lebesgue measure set of $\gamma$.

The form of Eq. (4) is obtained as follows. The factor $\phi(p)$ is the number of times the integer $p$ appears in the complete Farey tree (starting at the lowest level with $p_a = p_b = 1$). The factor $p2^{-p}$ is obtained from our numerical observations (and by direct analytical calculation in a special case) of how the width of an interval scales with the period $p$.

What is the character of the set $S_\gamma$ of $\gamma$ values for which the optimal orbit is nonperiodic? From the above discussion, $S_\gamma$ has zero Lebesgue measure. On the basis of our numerical evidence, we can show that $S_\gamma$ is a Cantor set (in particular, $S_\gamma$ is uncountable) whose fractal dimension is zero. Also, based on the Farey structure, we can show that when $\gamma \in S_\gamma$, the nonperiodic orbit that maximizes $\langle F_\gamma \rangle$ has topological entropy zero. The above arguments are deferred to a future, longer publication [10].

Based on our numerical results we make a general conjecture concerning typical maps with chaotic attractors and typical smooth optimization functions $F$ with a parameter dependence.

*Conjecture:* Optimal nonperiodic orbits occur on a set of zero Lebesgue measure in the parameter space of $F$.

In the remainder of this paper, we present some further numerical results involving different choices of the optimization function $F$ and different dynamical systems in support of the above conjecture and the principle that for most parameters, $\langle F \rangle$ is maximized by a low period orbit. Other cases appear in [10].

The fifth column of Table I shows the fraction of $10^5$ evenly spaced values of $\gamma$ for which a period $p$ orbit of the map (2) maximizes the average of a different function

$$F_\gamma(x) = \cos[2\pi(x - \gamma)] + \sin[6\pi(x - \gamma)]. \qquad (5)$$

The sixth column of Table I gives the corresponding fraction for the lowest $p$ within 90% of optimal. The function in Eq. (5) has three local maxima and three local minima. This increases the likelihood of a higher period orbit maximizing $\langle F_\gamma \rangle$, as is reflected in the data. The Farey structure, present for smooth functions with a single maximum [e.g., Eq. (3)], is found only partially in this case (and in the examples with two-dimensional maps that follow). Thus the number of intervals $\#(p)$ for which a period $p$ orbit maximizes $\langle F_\gamma \rangle$ is in general not equal to the Euler function $\phi(p)$. However, we find that the size of each period $p$ interval still tends to scale like $p2^{-p}$; if we replace the Euler functions $\phi(p)$ in Eq. (4) by the numerically observed number of $\gamma$ intervals $\#(p)$ for which a period $p$ orbit maximizes $\langle F_\gamma \rangle$, good agreement with Eq. (4) is restored. This is illustrated by the data represented as squares in Fig. 2. Another important point is that for Eq. (5) [as for Eq. (3)] we observe an exponential decrease, as a function of $p$, of the proportion of phase values $\gamma$ for which $\langle F_\gamma \rangle$ is maximized on an orbit of period at least $p$. Thus the results that low period orbits most often are optimal and that the conjecture holds are apparently independent of our choice of $F$.

The above discussion has been for a one-dimensional map. How do these results carry over into higher dimensionality? To get some indication of the situation we consider two different two-dimensional maps. First, we discuss the Kaplan-Yorke map [11],

$$x_{n+1} = 2x_n (\mathrm{mod}\ 1), \qquad (6a)$$

$$y_{n+1} = \lambda y_n + \frac{1}{\pi} \sin(2\pi x_n). \qquad (6b)$$

The Lyapunov exponents are $\ln 2$ and $\ln \lambda$. Choosing $\lambda = 0.4$ we have an information dimension of $D \approx 1.76$ for the attractor. Results for the optimal period with $F$ chosen to be

$$F_\gamma(x, y) = \cos[2\pi(x + y - \gamma)] \qquad (7)$$

are shown in the second and third columns of Table II. Also, the scaling of the average size of the $\gamma$ interval on which a given period $p$ orbit maximizes $\langle F_\gamma \rangle$ is shown by the triangles in Fig. 2. These results offer further support for our conjecture.

Next we consider the Hénon map

$$x_{n+1} = a + by_n - x_n^2, \qquad (8a)$$

$$y_{n+1} = x_n, \qquad (8b)$$

TABLE II. Numerical results 2D maps.

| | Kaplan-Yorke map (6) | | Hénon map (8) | |
|---|---|---|---|---|
| $p$ | $f(p)$ | $f_{90\%}(p)$ | $f(p)$ | $f_{90\%}(p)$ |
| 1 | 0.282 | 0.319 | 0.427 | 0.434 |
| 2 | 0 | 0 | 0.421 | 0.424 |
| 3 | 0 | 0 | 0 | 0 |
| 4 | 0.140 | 0.188 | 0.0862 | 0.0857 |
| 5 | 0.223 | 0.326 | 0 | 0 |
| 6 | 0.127 | 0.139 | 0.00823 | 0.0352 |
| 7 | 0.0768 | 0.0285 | 0.0415 | 0.0210 |
| 8 | 0.0466 | 0 | 0 | 0 |
| 9 | 0.0524 | 0 | 0 | 0 |
| 10 | 0.0162 | 0 | 0 | 0 |
| 11 | 0.0169 | 0 | 0 | 0 |
| 12 | 0.00518 | 0 | 0.00915 | 0 |
| 13 | 0.00750 | 0 | 0.00531 | 0 |
| 14 | 0.00274 | 0 | 0 | 0 |
| 15 | 0.00158 | 0 | 0 | 0 |
| 16–24 | 0.00214 | 0 | 0.00205 | 0 |

with the often studied parameter values $a = 1.4$, $b = 0.3$. The periodic orbits of this map were found using the method of [12], and the function we averaged was

$$F_\gamma(x, y) = \cos[(\pi/2)(x + y - \gamma)]. \tag{9}$$

The results are given in the fourth and fifth columns of Table II, and by the crosses in Fig. 2. Evidently the principle that the optimum is typically achieved by low period orbits, and that near optimum performance can always be achieved by such orbits, continues to hold.

Finally, we note that in all the cases above, the Farey tree structure we found in the prototype case of Eqs. (2) and (3) is still partially present. In the examples, Eqs. (5)–(9), we sometimes observe sudden transitions between $\gamma$ intervals corresponding to different low periods, but we still find that the high period $\gamma$ intervals are created by Farey summation (see [10]). The important point is that this implies the appearance of optimal nonperiodic orbits by the same Farey mechanism as for Eqs. (2) and (3), thus supporting our conjecture and indicating the general applicability of the behavior we observed for Eqs. (2) and (3).

We thank H. Kaplan, A. Lopes, D. Mauldin, M. Rychlik, J. Yorke, and L.-S. Young for helpful discussions. This research was supported by the U.S. Department of Energy (Offices of Scientific Computing and Energy Research), by the National Science Foundation (Divisions of Mathematical and Physical Sciences), and by the Office of Naval Research. The numerical computations reported in this paper were made possible by a grant from the W. M. Keck Foundation.

*Electronic address: bhunt@ipst.umd.edu

[1] E. Ott, C. Grebogi, and J. A. Yorke, Phys. Rev. Lett. **64**, 1196 (1990).

[2] J. C. Alexander, I. Kan, J. A. Yorke, and Z. You, Int. J. Bif. Chaos **2**, 795 (1992); E. Ott, J. C. Sommerer, J. C. Alexander, I. Kan, and J. A. Yorke, Phys. Rev. Lett. **71**, 4134 (1993); J. C. Sommerer and E. Ott, Nature (London) **365**, 136 (1993).

[3] E. Ott, J. C. Sommerer, J. C. Alexander, I. Kan, and J. A. Yorke, Physica (Amsterdam) **76D**, 384 (1994).

[4] Another related situation occurs in the "bubbling transition" [5,6] first noted by Ashwin, Buescu, and Stewart [5]. This transition is marked by the onset of temporally intermittent bursting in the presence of small noise [see Refs. [3,5] and the paper of N. Platt, S. M. Hammel, and J. F. Heagy, Phys. Rev. Lett. **72**, 3498 (1994)].

[5] P. Ashwin, J. Buescu, and I. Stewart, Phys. Lett. A **193**, 126 (1994).

[6] S. C. Venkataramani *et al.* (to be published); Y.-C. Lai *et al.* (to be published).

[7] J. A. Yorke (private communication) has suggested that the bifurcation is typically mediated by a periodic orbit, and this conjecture is supported by this paper.

[8] A different but related result has been obtained by B. R. Hunt and J. A. Yorke [Trans. Am. Math. Soc. **325**, 141 (1991)], who argue that a certain type of crisis bifurcation of a chaotic attractor is typically mediated by a low period unstable periodic orbit.

[9] This line of argument is supported by the work of K. Sigmund [Am. J. Math. **94**, 31 (1972)], who proved that for hyperbolic systems every invariant measure can be approximated arbitrarily well by the $\delta$-function measure on a periodic orbit.

[10] B. R. Hunt and E. Ott (to be published).

[11] J. L. Kaplan and J. A. Yorke, in *Functional Differential Equations and Approximation of Fixed Points,* edited by H.-O. Peitgen and H.-O. Walter, Lecture Notes in Mathematics Vol. 730 (Springer, Berlin, 1979), p. 204.

[12] O. Biham and W. Wenzel, Phys. Rev. Lett. **63**, 819 (1989); see also P. Grassberger, H. Kantz, and U. Moenig, J. Phys. A **22**, 5217 (1989).